A EUROPEAN JOURNAL OF CHEMICAL BIOLOGY

CHEMBIOCHEM

SYNTHETIC BIOLOGY & BIO-NANOTECHNOLOGY

Accepted Article

Title: A photoactivatable α5β1-specific integrin ligand

Authors: Aranzazu del Campo, Roshna V Nair, and Aleeza Farrukh

To be cited as: *ChemBioChem* 10.1002/cbic.201800180

Link to VoR: http://dx.doi.org/10.1002/cbic.201800180

A Journal of ChemPubSoc Europe

WILEY-VCH www.chembiochem.org

10.1002/cbic.201800180
WILEY-VCH

FULL PAPER

A photoactivatable $\alpha_5\beta_1$-specific integrin ligand

Roshna V. Nair,[a] Aleeza Farrukh,[a] Aranzazu del Campo*[a,b]

Abstract: The integrin $\alpha_5\beta_1$ is overexpressed in colon, breast, ovarian, lung and brain tumors and has been identified as key component in mechanosensing. In order to study how dynamic changes of $\alpha_5\beta_1$ engagement affect cellular behaviour, photoactivatable derivatives of $\alpha_5\beta_1$ specific ligands are presented in this article. A photoremovable protecting group (PRPG) was introduced into the ligand structure at a relevant position for integrin recognition. The presence of the chromophore temporally temporarily inhibited ligand bioactivity. Light exposure at cell-compatible dose efficiently cleaved the PRPG and restored functionality. The photoactive ligand had an azide end-functional group for covalent immobilization onto biomaterials via click chemistry. Selective cell response (attachment, spreading, migration) to the activated ligand on the surface is achieved upon controlled exposure, at similar levels to the native ligand. Spatial and temporal control of the cellular response is demonstrated, including the possibility to *in situ* activation. Photoactivatable integrin-selective ligands in model microenvironments will allow the study of cellular behavior in response to changes in the activation of individual integrins as consequence of dynamic variations of matrix composition.

Introduction

The interaction between membrane integrins and adhesive and structural proteins on the extracellular matrix (ECM) is fundamental in cellular processes like adhesion or migration.[1] Experimental investigation of these interactions is typically performed using anti-integrin monoclonal Antibodies[2] or peptidomimetics to block or activate individual integrins.[3] Out of 24 different integrin subtypes created by combinations of 18 α and 8 β subunits, almost half of them bind to ECM proteins through the tripeptide Arg-Gly-Asp (RGD), a widely represented adhesive motif in ECM proteins like fibronectin, vitronectin or collagen. Several groups have developed RGD-based ligands with high specificity for individual integrins,[4] Kessler's group being one of the major contributors with peptidomimetics with high affinity and selectivity towards $\alpha_5\beta_1$ and $\alpha_v\beta_3$ integrins,[5] recently expanded to epithelial integrin $\alpha_v\beta_6$.[5b] originally developed as antagonists for cancer therapeutics. These ligands have become unique tools to study integrin-mediated adhesion to matrices, and to investigate the individual role of $\alpha_5\beta_1$ and $\alpha_V\beta_3$ in cell adhesion and migration, as well as their involvement in mechanosensing and mechanotransduction.[6] For example, β_3 integrins have been demonstrated to favour persistent migration and β_1 integrins random migration in fibroblasts.[7] Fibrillar adhesion patterns and increased spreading are observed in cells attached to surface *via* $\alpha_5\beta_1$ ligands, whereas localized focal adhesion clusters at cell margins are obtained in cells adhering to $\alpha_v\beta_3$ ligand.[8] Activation of $\alpha_5\beta_1$-integrins is associated with high RhoA activity,[9] reduction in actin stress fiber formation and increase in cortical actin assembly.[10] Cells attached to surface through $\alpha_5\beta_1$ –integrins exert higher forces in comparison to cells spreading due to $\alpha_v\beta_3$ integrins.[8, 11] Also, $\alpha_5\beta_1$ –integrins are shown to enhance generation of cellular traction forces.[12] Both integrins crosstalk in mechanotransduction processes.[6c, 13] $\alpha_5\beta_1$ integrins are responsible for $\alpha_v\beta_3$ recruitment through an inside-out signaling. $\alpha_5\beta_1$ integrins are necessary for polarization and rigidity sensing of keratocytes after spreading *via* interaction of $\alpha_v\beta_3$ integrins.[14] All these experiments have been performed in static culture conditions, i.e. by exposing the cells to a predefined concentration of the ligand/s, and without the possibility of dynamic manipulation at later time points during cell culture. Dynamic changes of the ECM composition are, however, associated to physiologically and pathological states in which integrins are known to play relevant roles.[15] In order to mimic these scenarios *in vitro*, advanced strategies that allow on-demand activation or deactivation of the integrin ligand during cell culture are necessary. In the past, we successfully demonstrated a strategy to modulate the activity of the generic integrin binding ligand cyclic[RGDfK] by using light.[16]

[a] R. V. Nair, A. Farrukh, A. del Campo
INM – Leibniz Institute for New Materials, Campus D2 2,
66123 Saarbrücken, Germany
E-mail: Aranzazu.DelCampo@leibniz-inm.de
[b] A. del Campo
Saarland University,
Chemistry Department,
66123 Saarbrücken, Germany

Supporting information for this article is given via a link at the end of the document.((Please delete this text if not appropriate))

10.1002/cbic.201800180

FULL PAPER

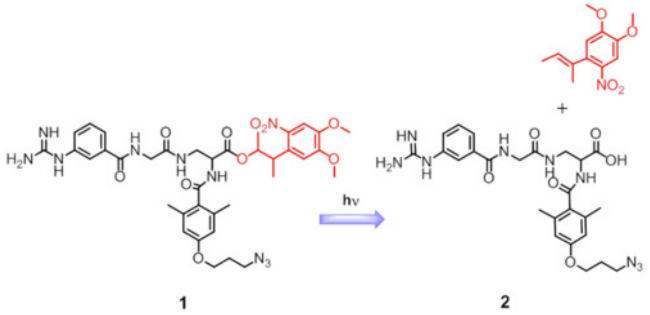

Scheme 1. Structure of phototriggerable $\alpha_5\beta_1$ specific ligand **1** and its photochemical activation reaction with photolysis products.

For this purpose, a photocleavable group was introduced at the carboxylic group of the aspartic acid in the peptide sequence.[16a] In this form, the peptide was inactive. Light exposure at cell compatible doses allowed *in situ*, remote and dose-dependent tuning of RGD bioactivity (through the photocleavage of the chromophore), with spatial and temporal control.[16b, 17] This was demonstrated in cell cultures and in vivo experiments.[18] However, RGDfK binds to many different integrins and does not allow dynamic integrin-selective studies. In this work, we extend this approach to control the activity of a variant of Kessler's $\alpha_5\beta_1$-specific integrin ligand (**2**, Scheme 1**)**. By attaching a 3-(4,5-Dimethoxy-2-nitrophenyl)-2-butyl ester (DMNPB) photocleavable group to the free carboxylic group, a phototriggerable derivative of **2** was obtained (**1**, Scheme 1). This molecule allows regulation of $\alpha_5\beta_1$ integrin related cellular processes by light exposure. This article describes the synthesis of the key molecule, and the demonstration of light-driven bioactivity in adhesion and migration assays.

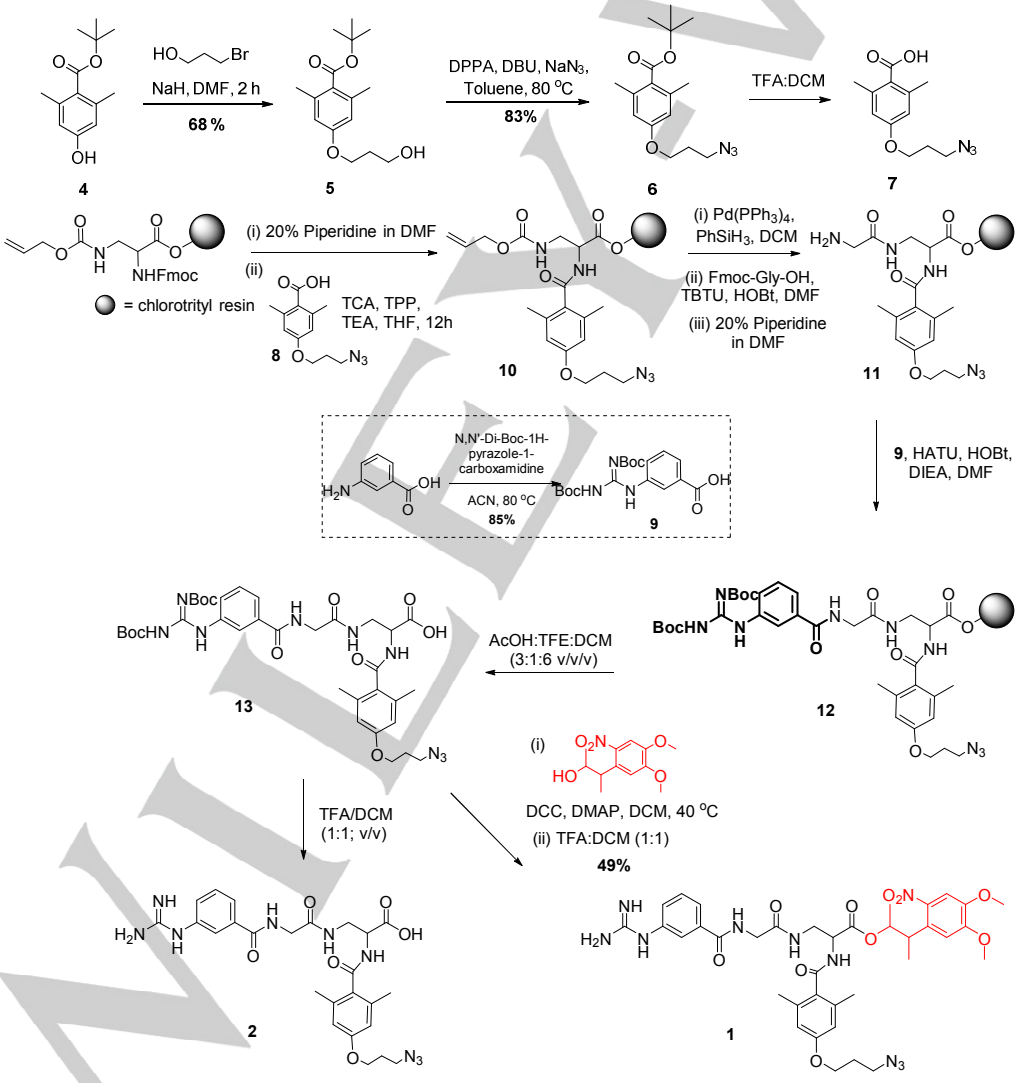

Scheme 2. Synthetic steps involved in preparation of **1** and **2**.

Results and Discussion

Synthesis of photoactivatable $\alpha_5\beta_1$ ligand with surface functionalisable azide group

The synthesis strategy for **1** and **2** was adapted from the method reported by Kessler group.[1] The ligands in this work contain azide groups for later coupling to biomaterials, in contrast to reported ligands from Kessler's group functionalized with thiols.[19] The azide group has reasonable stability against acidic or basic treatments and allows some simplification of protection steps during the synthesis of the molecule **1**.[19] The azide linker was introduced starting from Kessler's intermediate tert-butyl 4-hydroxy-2,6-dimethylbenzoate **4** in only 3 steps (details in Scheme 1 in SI): a simple S_N2 reaction with 1-bromopropanol, followed by azidation of hydroxyl group[20] and deprotection of *tert*-butyl ester. 4-(3-azidopropoxy)-2,6-dimethylbenzoic acid (**7**) was obtained in good yields. Coupling of **7** to Dap(Alloc) on chlorotrityl polystyrene (TCP) resin was performed following the strategy reported by Vágó and Greiner[21] using trichloroacetonitrile and triphenylphosphine in THF. This coupling required long reaction time (12 h), but proceeded to acceptable 60% conversion. The unreacted amines were capped using acetic anhydride. Attempts to couple **7** using agents like HATU, HBTU and PyBrOP were all unsuccessful, even in N-Methyl-2-pyrrolidone (NMP) and DMF as solvents. Attempts to couple 4-(3-(((benzyloxy)carbonyl)amino)propoxy)-2,6-dimethylbenzoic acid **10a** were also unsuccessful (details in SI, Table S1). For the following coupling steps on the resin, DMF was used as solvent and Kessler's conditions were used.[5b] Another deviation from Kessler`s method was the coupling of diBoc-protected guanidylated 3-aminobenzoic acid (**9**) to **11** to obtain **12** in simple coupling step. Kessler carried out the guanidylation reaction on the resin using dry chloroform as solvent.[5b] These reaction conditions did not work for the guanidylation of 3-amino benzoic acid for the synthesis of **9**. Instead, using dry acetonitrile afforded **9** with 80% yield at room temperature. The protected guanidine group was necessary in order to avoid interference with the coupling of the DMNPB group at later step. The cleavage of the molecule from the resin to obtain **13** with intact diBoc-protected guanidine group was a crucial step. The use of chlorotrityl resin (TCP) was necessary, as TCP allows cleavage the molecule from the resin under mild conditions. Reaction of **13** with 3-(4,5-Dimethoxy-2-nitrophenyl)-2-butyl ester (DMNPB) and subsequent deprotection of Boc groups of guanidine afforded the targeted molecule **1**. The active ligand **2** was easily obtained from **13** after deprotection step. The final products were isolated with high purity and characterized. Details on the synthetic protocols and characterization are provided in the supporting information, together with information about alternative routes taken for the synthesis of the intermediates.

Photochemical properties of photoactivatable $\alpha_5\beta_1$ ligand (1)

The photolysis of **1** in solution was followed by UV spectrophotometry and HPLC. A 0.5 mM solution of **1** in water was irradiated at λ_{max} = 360 nm (2.7 mW/cm^2) at increasing exposure times. The UV spectra showed a slight increase and broadening of the absorption maximum (λ_{max} = 346 nm) (Figure S1). This change is associated to the decreasing concentration of DMNPB and the increasing concentration of photolytic byproduct. Aliquots of 20 µL were taken at different time intervals and the composition of the irradiated mixture was analyzed by quantitative HPLC. The HPLC peak corresponding to **1** (t_r = 27.1 min) decreased in intensity (the peak at t_r = 27 min corresponds to photolysis side product) with increasing exposure time, while a new peak with increasing intensity appeared at t_R = 19.2 min. This peak showed absorption only in 210 nm and 254 nm channels, but not in 360 nm, indicating that DMNPB chromophore was not part of its structure (**Figure 1a**). Mass analysis confirmed that the new peak corresponded to the activated ligand **2**. In order to quantify the concentration of **2** liberated in the solution, a calibration curve was established and the area% of the peaks with tr = 19.2 min was interpolated. A conversion degree of 92% was measured at full exposure (**Figure 1b**). This high chemical yield and the clean photolysis reaction are relevant properties for a successful application of **1** in the following biological experiments.

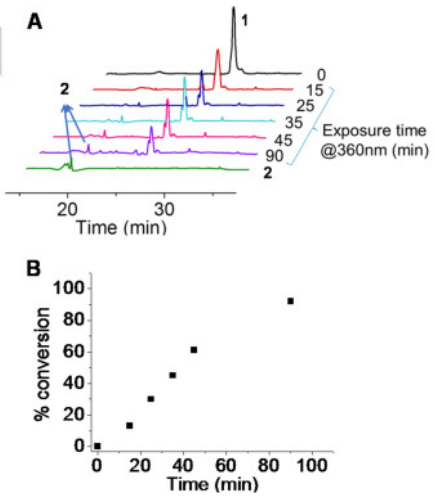

Figure 1. A HPLC profiles of a 0.5 mM solution of **1** in water at different exposure time at 360 nm (2.7 mW/cm^2). Elugrams were recorded with 210 nm channel in HPLC. **B** Conversion degree of the photolysis of **1**.

Bioactivity of photoactivatable $\alpha_5\beta_1$ ligand

In order to test the bioactivity of the synthesized ligands **1** and **2**, these were used to derivatize commercially available Nexterion® H slides for studies of cell responses. Nexterion H slides have NHS-activated carboxy-terminated PEGylated surfaces, which were converted into dibenzocyclooctyne (DBCO) groups by reaction with Dibenzocyclooctyne-amine in DMSO. Incubation of the substrates with compounds **1** or **2** is expected to click the ligands to the surface *via* copper-free azide-alkyne cycloaddition reaction.

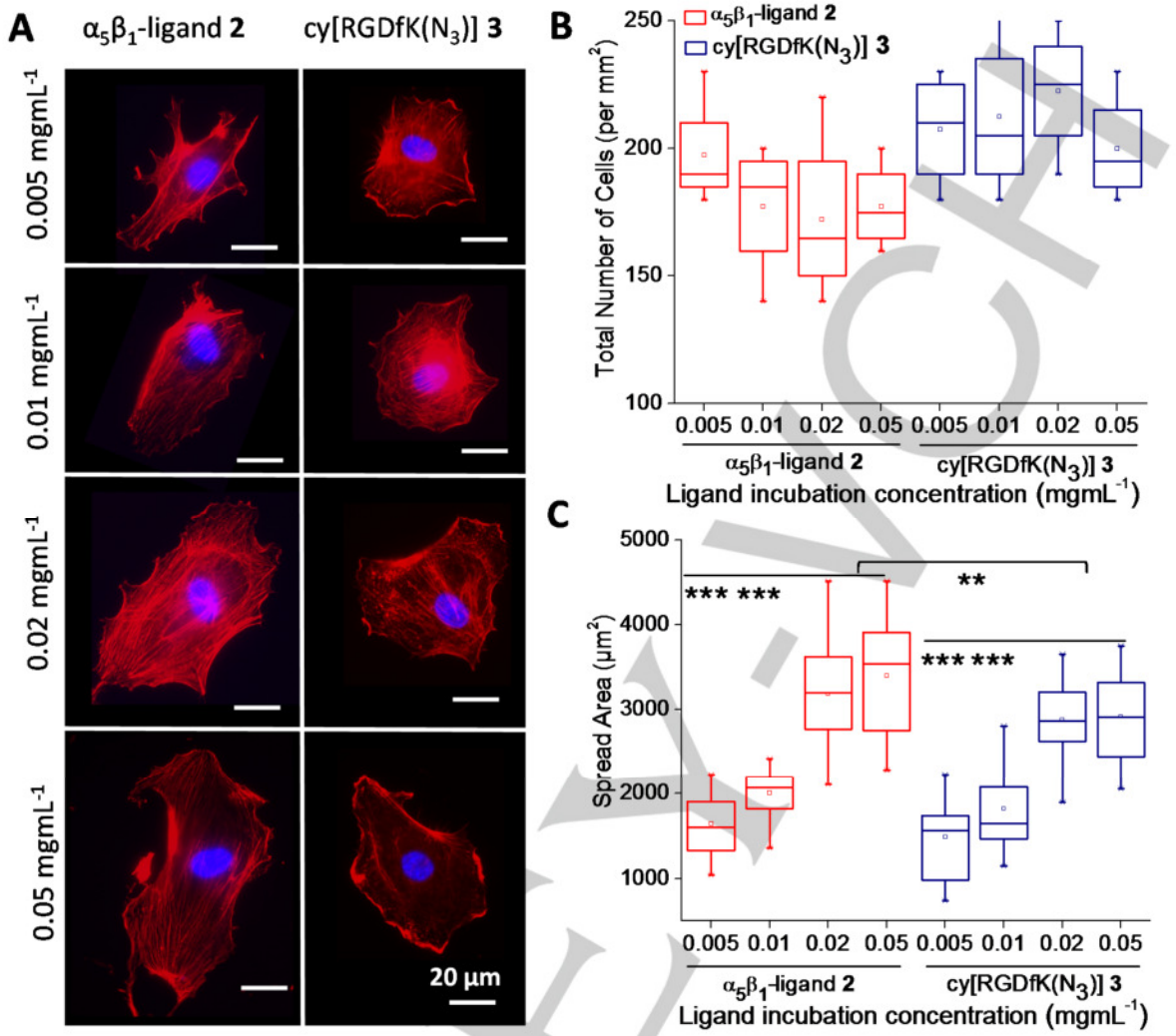

Figure 2. A. Immunofluorescence images of HUVECs after 24 h of culture on $\alpha_5\beta_1$-ligand **2** and cyclo[RGDfK(N_3)] **3** modified substrate at increasing ligand densities. Actin fibers were stained with Phalloidin TRITC and nucleus with DAPI. **B.** Quantification of the cell density on the surface. **C**. Quantification of cell spreading. Statistical significance was analyzed by Tukey- test shows significant differences between different concentrations and different ligands. Significance was calculated by comparison of difference concentrations to 0.05 mgmL^{-1}, and between the ligand in comparison with $\alpha_5\beta_1$-ligand (mean ± SD, ANOVA, ** p <0.01, *** p <0.001). No statistically significant difference was observed in total number of cells in all tested conditions. Quantification was performed by taking images from four independent experiments with at least 10 fields for each experimental condition at magnification of 0.22 µm per pixel (~350-400 cells were analyzed).

Initially different incubation concentrations of $\alpha_5\beta_1$-ligand 2 (0.005 – 0.05 mgmL^{-1}) were used in order to determine the optimal concentration to which cells respond. HUVECs were cultured on functionalized substrates for 24h, fixed and imaged. Cell attachment was observed on all substrates. The number of adhered cells per given area was not significantly different at the different ligand concentrations tested, and even showed a slight decrease at higher concentrations (Figure 2B). This decrease was associated with significant increase of spreading area observed for incubation concentrations above 0.02 mgmL^{-1} (Figure 2C). These results demonstrate that the exchange of the thiol linker by azide in Kessler's $\alpha_5\beta_1$ specific adhesive ligand[19] does not affect its activity.

Substrates modified with $\alpha_5\beta_1$-ligand **2** (0.02 mgmL^{-1} incubation concentration) were then taken for further studies, and cell behavior over time was observed by live cell imaging (**Figure 3A**). Within the first 15 minutes more than 60% of cells already attached on the substrate (**Figure 3C**), and significant spreading was visible within one hour (**Figure 3D**), indicating very fast cellular response to the ligand. Fast spreading kinetics was also reported for the thiol-derivatized ligand in Kessler's work.[5c, 7b, 19] The morphology of HUVECs quickly changed within the first 3h from circular to more elongated shape, and remained unchanged during rest of cell culture (**Figure 3A**).

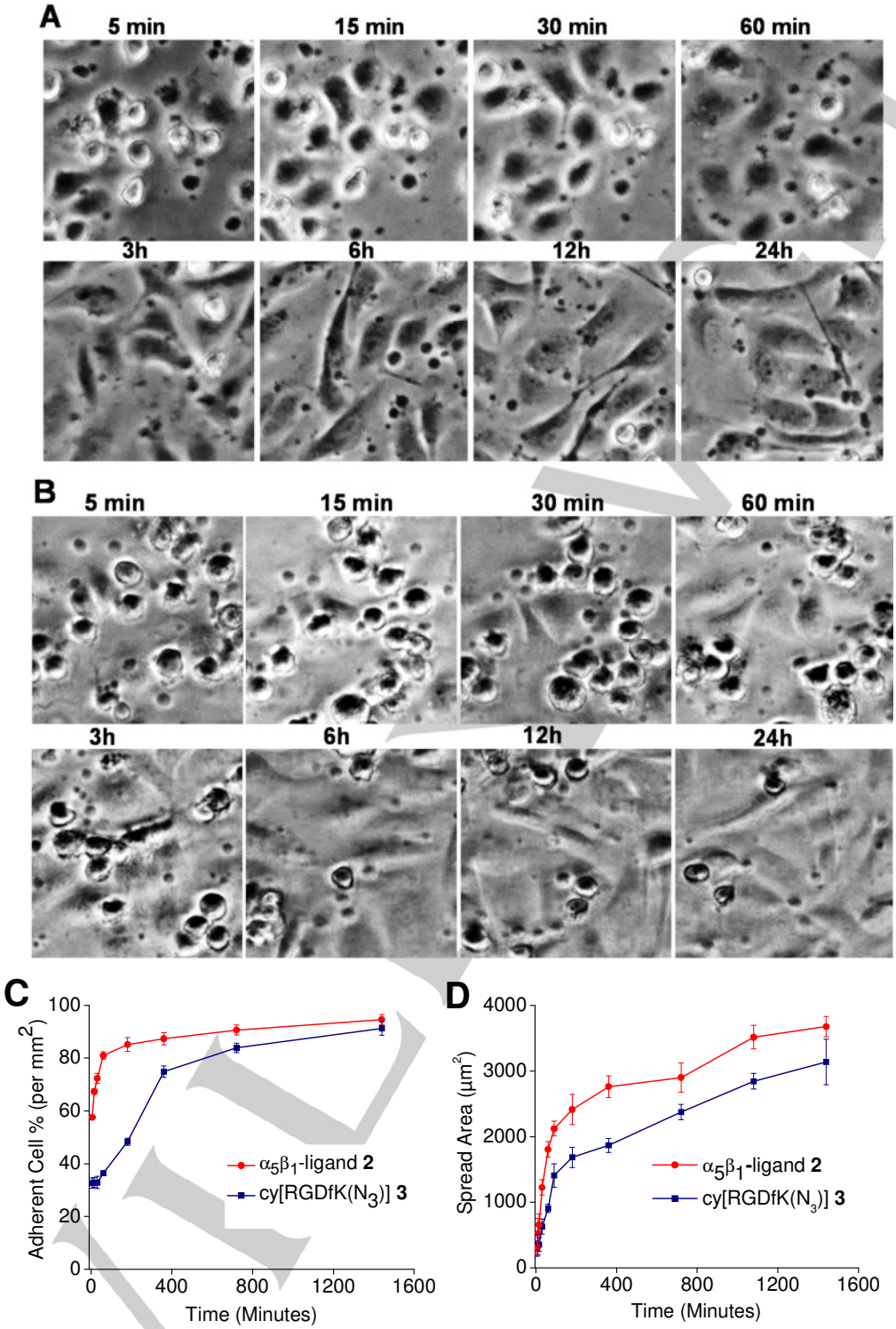

Figure 3. A, B: Phase contrast microscopy images of time lapse experiment over 24 hours showing the morphology of HUVECs cultured on Nexterion H slides functionalized with $\alpha_5\beta_1$-ligand **2** (A) or cy[RGDfK(N_3)] **3** (B) ligands (incubation concentration 0.02 mgmL^{-1}). **C, D:** Quantification of adherent cells and cell spreading area at different time points. Three independent experiments were performed and at least 10 images were taken for each experimental condition at 20x magnification for quantification. Spreading area was manually calculated by using area tool (contour) in Zen blue software (~300 cells were analyzed).

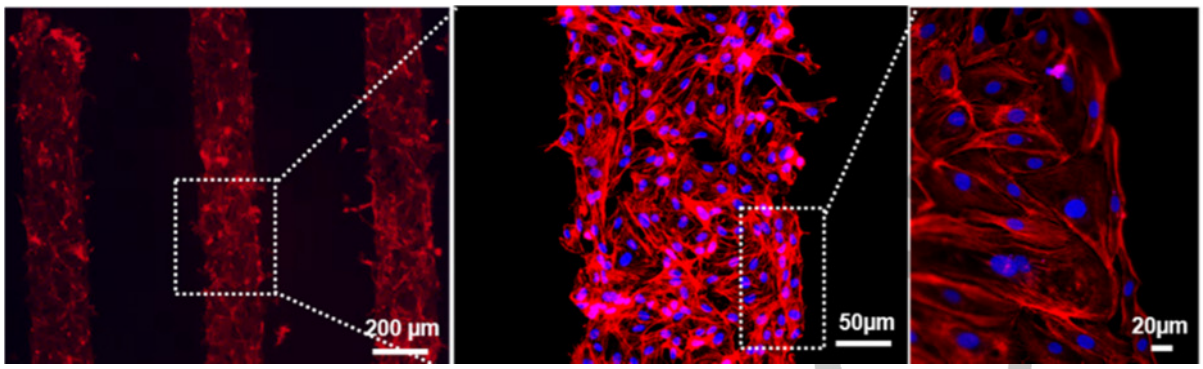

Figure 4. Site-selective adhesion of HUVECs on substrates functionalized with ligand **1** irradiated through quartz mask with 600 µm chrome stripe patterns separated by 300 µm gaps. HUVECs attach selectively to the exposed areas, where the ligand was activated. Images were taken 24 hours after seeding. Actin was stained with Phalloidin TRITC (red) and nucleus was stained with DAPI (blue).

For comparison, similar experiments were performed with the widely used RGD peptide motif using the azide-derivatized cyclo[RGDfK(N_3)] (**3,** structure in SI). This ligand binds to different integrins, including $\alpha_5\beta_1$. Cell attachment kinetics was significantly faster on $\alpha_5\beta_1$-ligand than on cy[RGDfK(N_3)]. A 40% higher number of adherent cells was measured on $\alpha_5\beta_1$-ligand after one hour of cell culture, though the difference vanished at longer culture times (Figure 3C). HUVECS show ~1 fold faster spreading on $\alpha_5\beta_1$-ligand than on cy[RGDfK(N_3)] during 1h of culture. This trend prevailed over 24h, when a 20% higher cell spreading was measured on $\alpha_5\beta_1$-ligand modified substrates (Figure 3D). Cells showed polarized and elongated morphology on $\alpha_5\beta_1$-ligand **2**, with more longitudinally oriented actin network in comparison to relatively randomly distributed actin fibers on cy[RGDfK(N_3)] (Figure 2A). These differences in the interaction of cells with $\alpha_5\beta_1$-specific ligand *vs* unspecific RGD motif reflect the different roles of integrins in adhesion.[8] These results foresee the possibility to manipulate cellular processes by regulating integrin-related signals using photoactivatable integrin-selective ligands.

The possibility to regulate the bioactivity of $\alpha_5\beta_1$-ligand **2** with the photoactivatable-$\alpha_5\beta_1$ variant **1** was then evaluated. HUVECs were seeded on substrates modified with photoactivatable-$\alpha_5\beta_1$ variant **1** (incubation concentration 0.02 $mgmL^{-1}$). No cell attachment was observed, indicating successful blocking of the binding site with the DMNPB chromophore and inhibition of integrin binding and integrin-mediated cell adhesion. On photoactivated samples, cells attached and spread in similar manner to positive controls (Figure S2). When substrates were irradiated trough a mask, cells selectively adhered to the exposed areas, with active $\alpha_5\beta_1$-ligand present now on the surface, forming well-defined patterns (Figure 4 and S3). The spatial selectivity was retained during 4 days of culture, demonstrating that **1** is stable against hydrolysis in cell culture conditions, and is photostable enough to allow culture under normal incubation conditions and during imaging. Cells on irradiated samples of functionalized with **1**, showed similar adhesion and spreading levels and kinetics to native $\alpha_5\beta_1$-ligand. All together, these results demonstrate that the introduction of the DMNPB photocleavable group at the carboxylic group of $\alpha_5\beta_1$ ligand temporary blocks the bioactivity of the ligand. The activity can be fully restored after light exposure.

Finally, the possibility to *in situ* activation of **1** in the presence of cells using a scanning laser was tested. Patterned monolayers of HUVECs (as in Figure 4) were placed in the cell chamber of a microscope, Using a scanning laser at 405 nm, lines of 40 µm width and 250 µm length were irradiated between the endothelial patterned monolayers. Note that these areas were not exposed in previous masked irradiation step and, therefore photoactivatable-$\alpha_5\beta_1$-ligand **1** was present in a latent form. Already 5 minutes after activation, migration of individual cells was observed along the scanned lines, confirming the *in situ* activation of the $\alpha_5\beta_1$ ligand. Cells detached from the monolayer and migrated along de line until they reached the other edge, approximately in 5h (Figure 5). Cell show fast migration into the activated area within the first 30 mins at 3 µm/min±0.5 speed, and persistent migration along the activated line at 0.6 µm/min±0.2 speed during the next 5.5 h. No cell retraction (change in the migration direction) was observed during cell culture (Figure S4).

Conclusions

In conclusion, a phototriggerable variant of $\alpha_5\beta_1$ antagonist with an azide terminated linker was successfully synthesized. The covalently attached DMNPB chromophore at the COOH group allowed inhibition of the biological activity of the ligand, and efficient photolysis and reactivation at cell compatible light doses. Masked-irradiated substrates modified with **1** allowed site-selective attachment of HUVECs to the photoactivated areas. Cell adhesion and spreading levels and kinetics were similar to those of native $\alpha_5\beta_1$ ligand, in agreement with the high photochemical yield observed on the HPLC studies of irradiated solutions. These results evidence the potential of photoactivatable-$\alpha_5\beta_1$-ligand **1** as tool to study $\alpha_5\beta_1$-dependent processes in cell biology by allowing precise control of its presence and concentration in time and space.

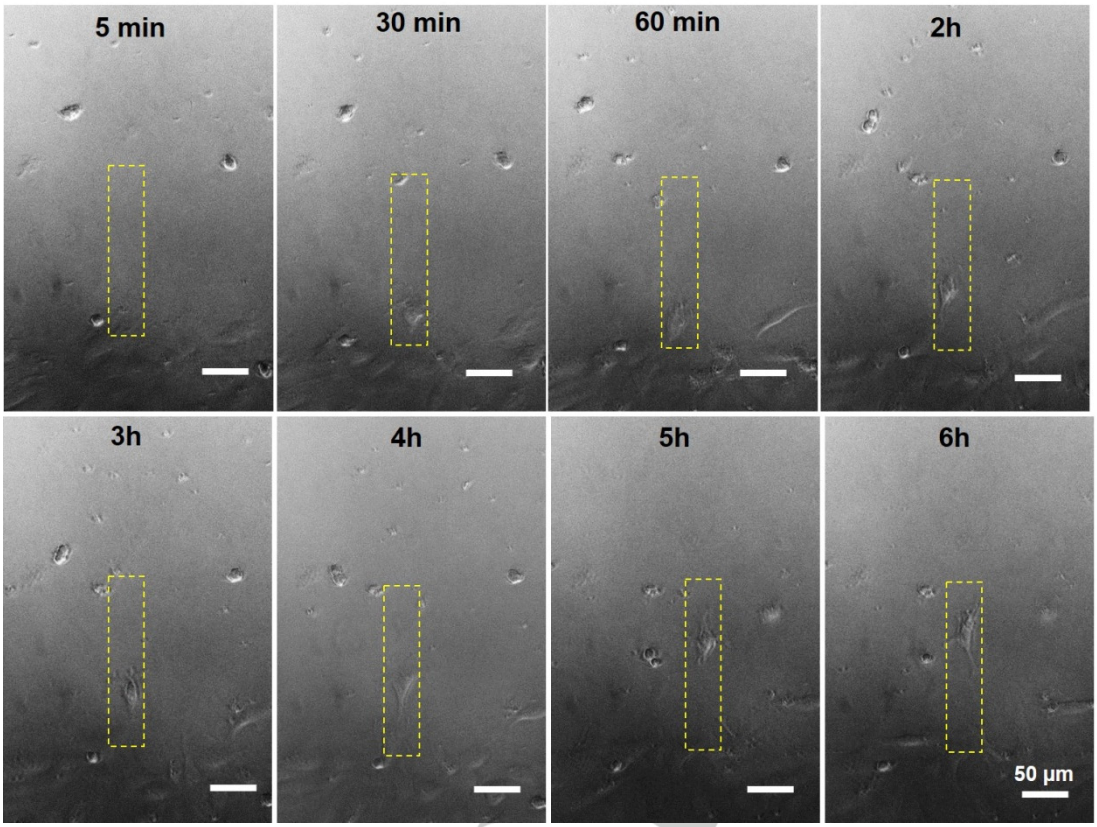

Figure 5. Light-triggered migration of HUVECs from the monolayer into $\alpha_5\beta_1$ activated lines using a scanning laser.

Experimental Section

Cell culture

Human umbilical vein endothelial cells (HUVECs) (Promocell) were cultured in M199 basal medium (Sigma, M4530) and supplemented with L-glutamine (2 mM), penicillin (1000 U/L), streptomycin (100 mg/L, Sigma), ECGS supplement (Sigma, E-2759), sodium heparin (Sigma, H-3393) and 20% fetal calf serum (FCS) as previously described.[16b] HUVEC were used between passages 2 to 6.

Nexterion® H glass slide functionalized with different concentration of ligand (photoactivatable-$\alpha_5\beta_1$-ligand 1, $\alpha_5\beta_1$-ligand **2** and cy[RGDfK(N_3)]) divided by 12-well silicon gasket, were seeded with 3×10^4 cells/well suspension of HUVECs at 37 °C and 5% CO_2. Cells were cultured for 24h and fixed with 4% PFA solution, permeabilized with 0.5% Triton, actin fibers were stained with TRITC-phalloidin (1:200) and DAPI (1:500) to stain nucleus the samples were mounted with mounting medium (Dinova) by using standard protocols. Fluorescence images were taken with Zeiss Axio Observer epi-fluorescence microscope.

Alternatively, samples were monitored by time-lapse microscopy for 24h by taking pictures every 5 min on Zeiss Axio observer microscope, equipped with CO_2 and heating unit.

For cell experiments of photoactivatable-$\alpha_5\beta_1$-ligand **1** functionalized samples without light activation, full pre-irradiation or irradiation through mask, 4×10^4 HUVECs were seeded/well. The medium was changed after 12 h to remove the unattached cells and cells were kept in culture till four days. Samples were fixed with 4% PFA solution and stained with TRITC-phalloidin and DAPI by using standard protocol as described above. Fluorescence images were taken with Zeiss Axio Observer epi-fluorescence microscope.

For *in-situ* photoactivation Zeiss Axio observer microscope, equipped with 405 nm RAPP® laser (100 mW cm^{-2}, 10% intensity, OD2 filter and 20X air objective) was used. Lines of 40 µm width and 250 µm length were activated next to monolayer of HUVECs by scanning for 30 seconds. Atleast 3 lines were scanned in each field of view.

Statistical Analysis

Data were expressed as mean ± standard deviation. For each condition, a minimum of three independent experiments were performed with sample size larger than 10 fields in all cases. The value of $p < 0.05$ was used for statistical significance. A one-way ANOVA with a Tukey test of the variance was used to determine the statistical significance between groups. The statistical significance difference was set to* $\alpha < 0.05$, **$\alpha < 0.01$, ***$\alpha < 0.001$.

Acknowledgements

AdC acknowledges funding from the European Union's Horizon 2020 research and innovation Program No. 731957 (FET Mechanocontrol) and from the Deutsche Forschungsgemeinschaft (SFB 1027). Authors thank Dr. Dimitri Missirlis (Heidelberg University) for fruitful discussions on the ligand activity.

Keywords: $\alpha_5\beta_1$ integrin • peptidomimetics • cell adhesive ligand • phototriggers.

[1] U. K. Marelli, F. Rechenmacher, T. R. Sobahi, C. Mas-Moruno, H. Kessler, *Front Oncol* **2013**, *3*, 222.

[2] A. Byron, J. D. Humphries, J. A. Askari, S. E. Craig, A. P. Mould, M. J. Humphries, *J. Cell Sci.* **2009**, *122*, 4009.

[3] A. Tolomelli, P. Galletti, M. Baiula, D. Giacomini, *Cancers* **2017**, *9*, 78.

[4] a K. Ley, J. Rivera-Nieves, W. J. Sandborn, S. Shattil, *Nat Rev Drug Discov* **2016**, *15*; bM. Pilkington-Miksa, E. M. V. Araldi, D. Arosio, L. Belvisi, M. Civera, L. Manzoni, *Org. Biomol. Chem.* **2016**, *14*, 3221-3233; cL. M. Miller, J. M. Pritchard, S. J. F. Macdonald, C. Jamieson, A. J. B. Watson, *J. Med. Chem.* **2017**, *60*, 3241-3251; dA. Sartori, E. Portioli, L. Battistini, L. Calorini, A. Pupi, F. Vacondio, D. Arosio, F. Bianchini, F. Zanardi, *J. Med. Chem.* **2017**, *60*, 248-262; eJ. M. Aizpurua, J. I. Ganboa, C. Palomo, I. Loinaz, J. Oyarbide, X. Fernandez, E. Balentova, R. M. Fratila, A. Jimenez, J. I. Miranda, A. Laso, S. Avila, J. L. Castrillo, *Chembiochem* **2011**, *12*, 401-405; fS. K. Narasimhan, P. Sejwal, S. Zhu, Y. Y. Luk, *Bioorg. Med. Chem.* **2013**, *21*, 2210-2216; gA. Tolomelli, L. Gentilucci, E. Mosconi, A. Viola, S. D. Dattoli, M. Baiula, S. Spampinato, L. Belvisi, M. Civera, *ChemMedChem* **2011**, *6*, 2264-2272.

[5] aT. G. Kapp, F. Rechenmacher, S. Neubauer, O. V. Maltsev, E. A. Cavalcanti-Adam, R. Zarka, U. Reuning, J. Notni, H.-J. Wester, C. Mas-Moruno, J. Spatz, B. Geiger, H. Kessler, *Sci. Rep.* **2017**, *7*, 39805; bD. Heckmann, A. Meyer, B. Laufer, G. Zahn, R. Stragies, H. Kessler, *Chembiochem* **2008**, *9*, 1397-1407; cC. Mas-Moruno, R. Fraioli, F. Rechenmacher, S. Neubauer, T. G. Kapp, H. Kessler, *Angew. Chem. Int. Ed.* **2016**, *55*, 7048-7067.

[6] aN. Wang, *Nat. Mater.* **2017**, *16*, 1173-1174; bN. Strohmeyer, M. Bharadwaj, M. Costell, R. Fässler, D. J. Müller, *Nat. Mater.* **2017**, *16*, 1262; cP. Roca-Cusachs, N. C. Gauthier, A. Del Rio, M. P. Sheetz, *Proc Natl Acad Sci U S A* **2009**, *106*, 16245-16250; dA. Elosegui-Artola, E. Bazellieres, M. D. Allen, I. Andreu, R. Oria, R. Sunyer, J. J. Gomm, J. F. Marshall, J. L. Jones, X. Trepat, P. Roca-Cusachs, *Nat. Mater.* **2014**, *13*, 631-637; eB. D. Matthews, D. R. Overby, R. Mannix, D. E. Ingber, *J. Cell Sci.* **2006**, *119*, 508-518; fH. E. Balcioglu, H. van Hoorn, D. M. Donato, T. Schmidt, E. H. Danen, *J. Cell Sci.* **2015**, *128*, 1316-1326.

[7] aD. Missirlis, T. Haraszti, H. Kessler, J. P. Spatz, *Sci. Rep.* **2017**, *7*, 3711; bD. Missirlis, T. Haraszti, C. v. C. Scheele, T. Wiegand, C. Diaz, S. Neubauer, F. Rechenmacher, H. Kessler, J. P. Spatz, *Sci. Rep.* **2016**, *6*, 23258.

[8] V. Schaufler, H. Czichos-Medda, V. Hirschfeld-Warnecken, S. Neubauer, F. Rechenmacher, R. Medda, H. Kessler, B. Geiger, J. P. Spatz, E. A. Cavalcanti-Adam, *Cell Adh. Migr.* **2016**, *10*, 505-515.

[9] E. H. J. Danen, P. Sonneveld, C. Brakebusch, R. Fässler, A. Sonnenberg, *J. Cell Biol.* **2002**, *159*, 1071-1086.

[10] aJ. Guasch, B. Conings, S. Neubauer, F. Rechenmacher, K. Ende, G. Rolli Claudio, C. Kappel, V. Schaufler, A. Micoulet, H. Kessler, H. G. Boyen, A. Cavalcanti - Adam Elisabetta, P. Spatz Joachim, *Adv. Mater.* **2015**, *27*, 3737-3747; bK. Burridge, C. Guilluy, *Exp. Cell Res.* **2016**, *343*, 14-20.

[11] S. Rahmouni, A. Lindner, F. Rechenmacher, S. Neubauer, A. Sobahi Tariq Rashad, H. Kessler, A. Cavalcanti - Adam Elisabetta, P. Spatz Joachim, *Adv. Mater.* **2013**, *25*, 5869-5874.

[12] G. L. Lin, D. M. Cohen, R. A. Desai, M. T. Breckenridge, L. Gao, M. J. Humphries, C. S. Chen, *FEBS Lett.* **2013**, *587*, 763-769.

[13] A. Katsumi, A. W. Orr, E. Tzima, M. A. Schwartz, *J. Biol. Chem.* **2004**, *279*, 12001-12004.

[14] M. Riaz, M. Versaevel, D. Mohammed, K. Glinel, S. Gabriele, *Sci. Rep.* **2016**, *6*, 34141.

[15] A. Starchenko, R. Graves-Deal, Y.-P. Yang, C. Li, R. Zent, B. Singh, R. J. Coffey, *Mol. Biol. Cell* **2017**, *28*, 1288-1300.

[16] aS. Petersen, J. M. Alonso, A. Specht, P. Duodu, M. Goeldner, A. del Campo, *Angew. Chem., Int. Ed.* **2008**, *47*, 3192-3195; bM. J. Salierno, A. J. García, A. del Campo, *Adv. Funct. Mater.* **2013**, *23*, 5974-5980; cM. Wirkner, S. Weis, V. San Miguel, M. Álvarez, R. A. Gropeanu, M. Salierno, A. Sartoris, R. E. Unger, C. J. Kirkpatrick, A. del Campo, *ChemBioChem* **2011**, *12*, 2623-2629.

[17] A. Specht, F. Bolze, Z. Omran, J. F. Nicoud, M. Goeldner, *HFSP J* **2009**, *3*, 255-264.

[18] T. T. Lee, J. R. García, J. I. Paez, A. Singh, E. A. Phelps, S. Weis, Z. Shafiq, A. Shekaran, A. del Campo, A. J. García, *Nat. Mater.* **2014**, *14*, 352.

[19] F. Rechenmacher, S. Neubauer, J. Polleux, C. Mas-Moruno, M. De Simone, E. A. Cavalcanti-Adam, J. P. Spatz, R. Fassler, H. Kessler, *Angew. Chem. Int. Ed.* **2013**, *52*, 1572-1575.

[20] A. S. Thompson, G. R. Humphrey, A. M. DeMarco, D. J. Mathre, E. J. J. Grabowski, *J. Org. Chem.* **1993**, *58*, 5886-5888.

[21] I. Vágó, I. Greiner, *Tet. Lett.* **2002**, *43*, 6039-6041.

10.1002/cbic.201800180